



HAL
open science

The significant role of water in reactions occurring on the surface of interstellar ice grains: Hydrogenation of pure ketene $\text{H}_2\text{C}=\text{C}=\text{O}$ ice versus hydrogenation of mixed $\text{H}_2\text{C}=\text{C}=\text{O}/\text{H}_2\text{O}$ ice at 10 K

Mohamad Ibrahim, Jean-Claude Guillemin, Patrick Chaquin, Alexis Markovits, Lahouari Krim

► To cite this version:

Mohamad Ibrahim, Jean-Claude Guillemin, Patrick Chaquin, Alexis Markovits, Lahouari Krim. The significant role of water in reactions occurring on the surface of interstellar ice grains: Hydrogenation of pure ketene $\text{H}_2\text{C}=\text{C}=\text{O}$ ice versus hydrogenation of mixed $\text{H}_2\text{C}=\text{C}=\text{O}/\text{H}_2\text{O}$ ice at 10 K. *Physical Chemistry Chemical Physics*, 2024, *Physical Chemistry Chemical Physics*, 26 (5), pp.4200-4207. <10.1039/d3cp04601j>. <hal-04443301>

HAL Id: hal-04443301

<https://hal.science/hal-04443301v1>

Submitted on 10 Nov 2024

HAL is a multi-disciplinary open access archive for the deposit and dissemination of scientific research documents, whether they are published or not. The documents may come from teaching and research institutions in France or abroad, or from public or private research centers.

L'archive ouverte pluridisciplinaire HAL, est destinée au dépôt et à la diffusion de documents scientifiques de niveau recherche, publiés ou non, émanant des établissements d'enseignement et de recherche français ou étrangers, des laboratoires publics ou privés.



HAL Authorization

The significant role of water in reactions occurring on the surface of interstellar ice grains: Hydrogenation of pure ketene $\text{H}_2\text{C}=\text{C}=\text{O}$ ice versus hydrogenation of mixed $\text{H}_2\text{C}=\text{C}=\text{O}/\text{H}_2\text{O}$ ice at 10 K

Mohamad Ibrahim¹, Jean-Claude Guillemin², Patrick Chaquin³, Alexis Markovits³ and Lahouari Krim^{1*}

¹*Sorbonne Université, CNRS, De la Molécule aux Nano-Objets: Réactivité, Interactions, Spectroscopies, MONARIS, 75005, Paris, France.*

²*Univ Rennes, Ecole Nationale Supérieure de Chimie de Rennes, CNRS, ISCR – UMR6226, F-35000 Rennes, France.*

³*Sorbonne Université, CNRS, Laboratoire de Chimie Théorique, LCT, 75005, Paris, France.*

**Corresponding author: Lahouari.krim@Sorbonne-universite.fr*

Abstract

Water ice plays an important role in reactions taking place on the surface of interstellar ice grains, ranging from catalytic effects that reduce reaction barrier heights to effects that stabilize the reaction products and intermediates formed, or that favor one reaction pathway over another, passing through water-involvement in the reaction to produce more complex molecules that cannot be formed without water or water-derived fragments H, O and OH. In this context, we have combined experimental and theoretical studies to investigate ketene (CH_2CO) + H solid-state reaction at 10 K in the presence and absence of water molecules under interstellar conditions, through H-bombardment of CH_2CO and $\text{CH}_2\text{CO}/\text{H}_2\text{O}$ ices. We show in the present study that with or without water, ketene molecule reacts with H atoms to form four reaction products, namely CO, H_2CO , CH_4 and CH_3CHO . Based on the amounts of CH_2CO consumed during the hydrogenation processes, the $\text{CH}_2\text{CO} + 2\text{H}$ reaction appears to be more efficient in the presence of water. This underlines the catalytic role of water ice in reactions occurring on the surface of interstellar ice grains. However, if we refer to the yields of reaction products formed during the hydrogenation of CH_2CO and $\text{CH}_2\text{CO}/\text{H}_2\text{O}$ ices, we find that water molecules favor the reaction pathway to form CH_3CHO and deactivate that leading CH_4 and H_2CO . These experimental results are in good agreements with the theoretical predictions that highlight the catalytic effect of H_2O on the $\text{CH}_2\text{CO} + \text{H}$ reaction, whose potential energy barrier drops from 4.6 kcal/mol (without water) to 3.8 and 3.6 kcal/mol with one and two water molecules respectively.

1. Introduction

The prebiotic building blocks detected or sought in the interstellar medium (ISM) play a fundamental role as building blocks of biological molecular complexes. In recent years, astrochemical and astrophysical research has focused on understanding the mechanisms of formation and evolution of these prebiotic building blocks in the ISM. The ketene molecule (CH_2CO) is one of the simple organic species of astrophysical interest that plays an important role in prebiotic astrochemistry and has been the subject of several observational, experimental and theoretical studies¹⁻⁹. Its detection was first proposed in Sagittarius B2 (SgrB2)¹⁰ in the 1970s, then confirmed and extended to translucent clouds¹¹⁻¹³, TMC-1, L183, prestellar core¹⁴ and extragalactic sources¹⁵. Organic species such as ketene can form and chemically evolve on the surface of water ices covering interstellar grains. However, amorphous solid water (ASW) is the most abundant water ice in the Universe and is ubiquitous in the ISM. In this context, a number of previous theoretical and experimental studies have focused on the role of water ice in the reaction processes that manage the chemistry of the interstellar medium, concentrating on photochemistry or radical reactions in interstellar ice analogues. Moore and Hudson¹⁶ studied the effect of H_2O concentration on CH_4 chemistry during proton bombardment at 10 K. They found that increasing the water content in the H_2O - CH_4 mixed ice leads to an increase in the production of oxidized species such as CH_3OH , CH_3CHO and $\text{CH}_3\text{CH}_2\text{OH}$, and a decrease in the formation of reduced species such as C_2H_6 . Krim et al¹⁷ studied the influence of H_2O on the VUV photochemistry of CH_3OH in the solid phase. They showed that the irradiations of CH_3OH ice and the H_2O : CH_3OH ice mixture lead to the production of H_2CO , CO , CO_2 , CH_4 and $\text{OHCH}_2\text{-CH}_2\text{OH}$ as the main photoproducts, with a production of CO_2 , H_2CO and CO strongly favored when CH_3OH is diluted in water. The production of H_2CO is increased by the reaction $\text{CH}_2\text{OH} + \text{H}_2\text{O}$, while that of CO_2 is increased by the reaction $\text{CO} + \text{OH}$. This shows that water and even fragments of water can be involved to a greater or lesser extent in the chemistry of the ISM. Oberg et al. investigated the effect of water concentration on the photochemistry¹⁸ of more volatile species, in particular CH_4 , showing that H_2O favors oxygen-rich products such as CH_3OH and H_2CO , as well as efficient trapping of the radicals formed in the ice. Pirim and Krim¹⁹ carried out the hydrogenation of pure CO ices, after which the CO concentration was progressively reduced and replaced by H_2O molecules. They showed that H_2O molecules favors the H-addition process over the H-abstraction reaction for the second stage of CO hydrogenation, thus leading to the production of CH_3OH . Jonusas and Krim²⁰ have shown that

the photolysis of $\text{NH}_3\text{-H}_2\text{O}$ ice leads to NH_2 and NH_2OH as the main photoproducts, the formation of which is catalyzed by water molecules, and that the photochemical reaction is highly dependent on the temperature and environment in which NH_3 and H_2O are trapped. Bulak et al.²¹ performed the VUV photolysis of CH_3CN ices to investigate the formation of larger nitrogen containing organic molecules such as $\text{CH}_3\text{CH}_2\text{CN}$, NCCN/CNCN and $\text{NCCH}_2\text{CH}_2\text{CN}$. They have also shown that the photolysis of mixed $\text{H}_2\text{O}:\text{CH}_3\text{CN}$ ices leads to the formation of species with different functional groups such as imines, amines, amides, large nitriles, carbocyclic acids and alcohols. From a theoretical calculation point of view, the isomerization of trans-HCOH to H_2CO in the presence of a water molecule was carried out using electronic structure calculations²². The presence of water molecules leads to a drastic reduction in the activation energy of at least 80% in the process of isomerizing trans-HCOH to H_2CO . This shows the significant role of water in reactions occurring on the surface of interstellar ice grains. Another theoretical study also highlights the catalytic role of water molecules, showing the possible formation of glycine from the reaction $\text{CH}_2=\text{NH} + \text{CO} + \text{H}_2\text{O}$. This study carried out by Nhlabatsi et al.²³ shows that by increasing the number of water molecules to three or more, the height of the activation barrier leading to the reaction exit pathway is reduced to such an extent that the transition state is more stable than that of the reactants. In addition, using quantum mechanical calculations, Darla et al.²⁴ studied the formation of formamide from $\text{HCN} + 2\text{H}_2\text{O}$, analyzing the role of the second water molecule from three different points of view, as catalyst, spectator and reactant. Due to the catalytic effect of the water, the height of the barrier in the reaction pathway is reduced and proved to be lower than that of the reactants $\text{HCN} + \text{H}_2\text{O}$. Water as a spectator does not radically affect the energy of the reaction $\text{HCN} + \text{H}_2\text{O}$, but it does stabilize the products formed. Finally, as a reactant, the second H_2O molecule takes part in the $\text{HCN}+\text{H}_2\text{O}$ reaction to produce the geminal-diol intermediate, which then leads to formamide as final product. The formation of complex organic molecules on various ices has been studied theoretically, such as glycine, formamide and other nitrogen containing molecules. Also, a sequence of reaction allowing the formation of ethanal starting from CCO on a CO rich ice has been recently published²⁵⁻²⁹.

Recently, our group have investigated the hydrogenation reaction of ketene ice³⁰ at 10 K, showing that the reaction $\text{CH}_2\text{CO} + \text{H}$ in the solid state leads to the formation of carbon monoxide (CO), methane (CH_4), formaldehyde (H_2CO) and acetaldehyde (CH_3CHO). In the present study, we focus on the influence of H_2O molecules on the hydrogenation of CH_2CO . In order to describe the role of water ice in the hydrogenation of CH_2CO , we compare the

results of experiments on $\text{CH}_2\text{CO} + \text{H}$ binary mixtures with those on $\text{CH}_2\text{CO} + \text{H} + \text{H}_2\text{O}$ ternary mixtures, in the solid phase at 10 K.

2. Experimental and calculation methods

The experimental set-up used in this study has been described in detail previously^{30,31}. Briefly, the experiments are carried out under ultra high vacuum at 10^{-10} mbar. The $\text{CH}_2\text{CO}/\text{H}_2\text{O}$ sample were prepared by co-condensation of CH_2CO and H_2O on a cryogenic metal mirror maintained at 10 K using a pulsed tube closed-cycle cryogenerator (Sumitomo cryogenics F-70) and programmable temperature controller (Lakeshore 336). Ketene, produced by thermolysis of acetic anhydride at 900°C , is preserved under vacuum in a large trap maintained at -196°C with liquid nitrogen. Controlled evaporation of the ketene in the injection ramp is ensured by a cooling bath consisting of ethanol and liquid nitrogen maintained at -110°C . Ketene vapor pressures in the injection ramp are measured using a digital Pirani gauge, while the fractions of ketene gas injected into the experimental chamber are controlled using a leak valve. In order to study the influence of water on the of CH_2CO hydrogenation reaction, two different experiments were carried out:

Hydrogenation of pure CH_2CO ice: As a reference experiment to investigate the $\text{CH}_2\text{CO} + \text{H}$ surface reaction, CH_2CO ices are formed at 10 K and then bombarded with H-atoms.

Hydrogenation of $\text{CH}_2\text{CO}/\text{H}_2\text{O}$ ice: $\text{CH}_2\text{CO}/\text{H}_2\text{O}$ ices are formed at 10 K and then bombarded with H-atoms. The sample is prepared by co-condensing $\text{CH}_2\text{CO}/\text{H}_2\text{O}$ mixtures onto a substrate at 10 K with a mixing ratio = 4. However the real mixing ratio is deduced from calculations of column densities of CH_2CO and H_2O in the resulting solid sample.

Atomic hydrogen is produced by a microwave driven atom source (SPECS PCR-ECS). This source uses a microwave discharge to generate gaseous plasma in a chamber supplied with molecular hydrogen. The resulting H/H_2 mixture, a combination of both atomic and molecular hydrogen (H/H_2) with a dissociation yield of 15%, is injected in the reaction chamber at a pressure of 10^{-5} mbar with an H-atom flux calculated around 1×10^{15} atoms $\text{cm}^{-2} \text{s}^{-1}$. All the ice samples with or without hydrogenation treatment are probed by infrared spectroscopy in the transmission-reflection mode between 5000 and 500 cm^{-1} , with a resolution of 0.5 cm^{-1} , using a Bruker 120 FTIR spectrometer.

For the theoretical part, for the $\text{CH}_2\text{CO} + \text{H}$ reaction in the presence of one or two water molecules, geometry optimizations were performed at the MP2/cc-pvtz level, followed by

single point CCSD(T) energy calculations. Potential energy barriers ~~Activation energies~~ were not ZPE corrected. The interaction geometries of CH₃CO with ketene or water were optimized at the B3LYP/cc-pvtz level, with a MP2 single point energy calculation. The Gaussian 09 series of programs³² was used throughout this work.

3. Results

In order to highlight the specific role of water in the hydrogenation process of solid ketene under ISM conditions, we first present the results of our reference experiment in which pure ketene ice is deposited and then bombarded by H-atoms in the absence of water molecules. Figures 1.a and 1.b show the infrared spectra of solid ketene at 10 K before and after H-bombardment, respectively. The IR signatures of solid CH₂CO are characterized by a very intense signal at 2114 cm⁻¹ corresponding to the C=O stretching mode, two signals at 3143 and 3041 cm⁻¹ attributed to the CH stretching modes, a signal at 1129 cm⁻¹ characteristic of the C=C stretching mode and by two other IR signals corresponding to the CH₂ bending and rocking modes detected around 1370 and 970 cm⁻¹, respectively^{33,34}. After H-bombardment of CH₂CO ice at 10 K, several products are observed through their characteristic fingerprints: formaldehyde^{35,36} (H₂CO) at 1720 and 1500 cm⁻¹, methane^{37,38} (CH₄) at 1304 and 3009 cm⁻¹, carbon monoxide³⁹ (CO) at 2136 cm⁻¹ and acetaldehyde (CH₃CHO) at 1351 and 1718 cm⁻¹.

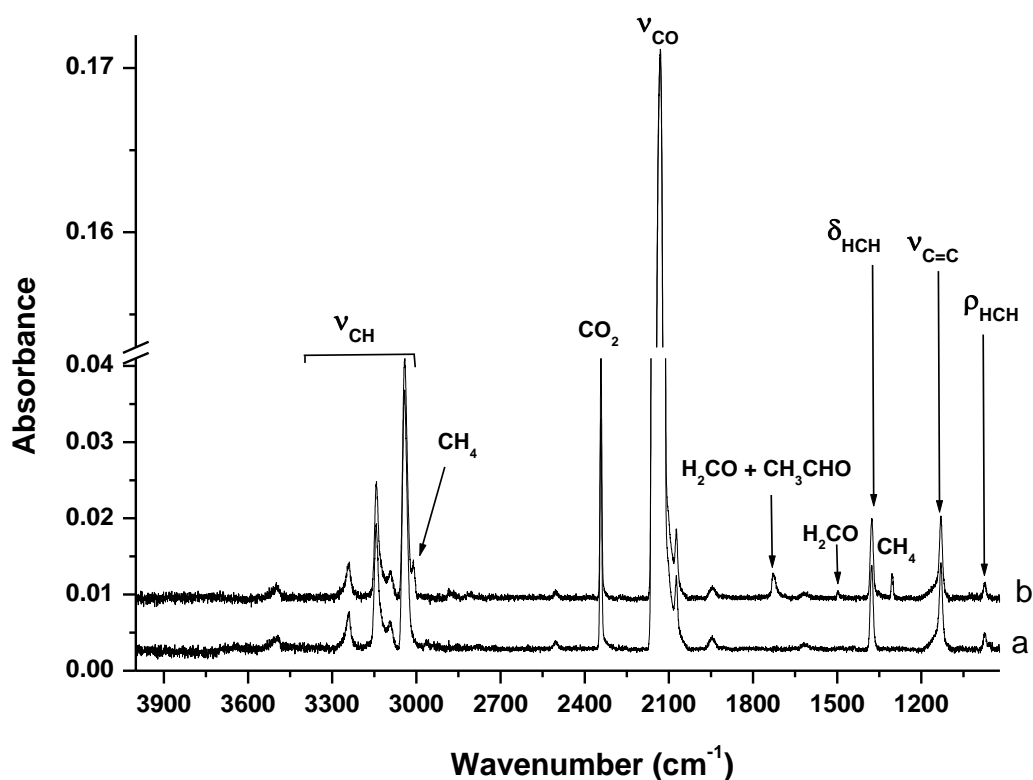
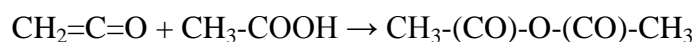
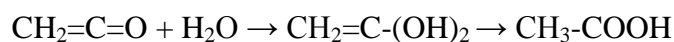


Figure 1: a) IR spectrum of ketene ice formed at 10 K. b) IR spectrum of ketene ice after H-bombardments. (ν , ρ and δ refer to the stretching, rocking and bending modes, respectively).

Figures 2a and 2b show the IR spectra of pure CH_2CO and $\text{CH}_2\text{CO}/\text{H}_2\text{O}$ ices formed at 10 K, respectively, in the spectral region between 2200 and 900 cm^{-1} . The IR spectrum of the $\text{CH}_2\text{CO}/\text{H}_2\text{O}$ ice in Figure 2a is characterised by a broad absorption band at 1600 cm^{-1} due to H_2O and by four IR signals, also observed in Figure 2b, which are attributable to CH_2CO . However, the IR spectrum of the $\text{CH}_2\text{CO}/\text{H}_2\text{O}$ ice also shows new IR signals around 1827, 1801, 1737, 1437, 1050 and 1000 cm^{-1} which cannot be attributed to either H_2O or CH_2CO but to a product from $\text{H}_2\text{O} + \text{CH}_2\text{CO}$ reaction which takes place in the ~~ramp~~ injection line before the $\text{CH}_2\text{CO}/\text{H}_2\text{O}$ mixture is introduced into the reaction chamber. Kahan et al.⁴⁰ have shown that in gas-phase, the presence of water vapor at 295 K with ketene lead to acetic acid acetic anhydride:



The first stage of the reaction is the formation of $\text{CH}_3\text{-COOH}$ by the interaction between ketene and water. Then $\text{CH}_3\text{-COOH}$ may react with additional CH_2CO to form anhydride acetic acid ($\text{CH}_3\text{COOCOCH}_3$). Based on this observation, we recorded the IR spectrum of the acetic anhydride (Figure 2c) and we note that all the new signals we observe in the IR spectrum of the $\text{CH}_2\text{CO}/\text{H}_2\text{O}$ ice correspond exactly to the IR signatures of $\text{CH}_3\text{COOCOCH}_3$.

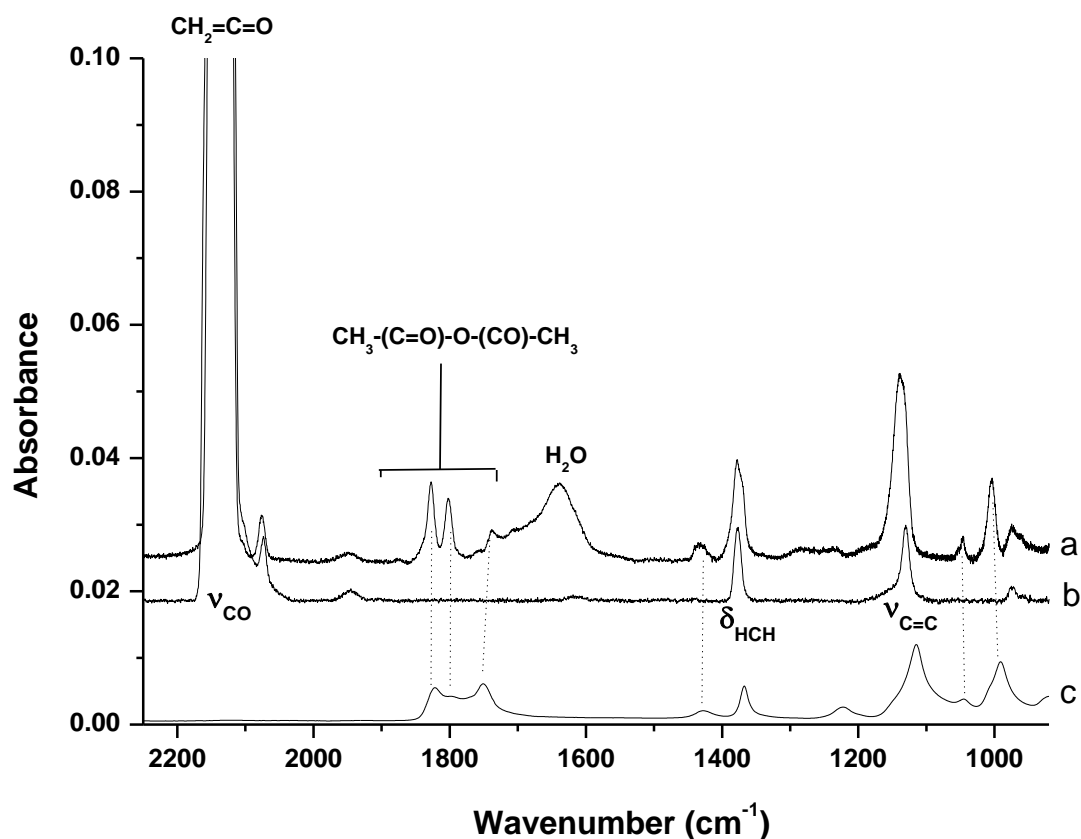


Figure 2: IR spectrum of a) $\text{CH}_2\text{CO}/\text{H}_2\text{O}$ ice formed at 10 K. b) CH_2CO ice formed at 10 K. c) Reference spectrum of acetic anhydride ($\text{CH}_3\text{COOCOCH}_3$) recorded at room temperature.

Before presenting the results of the $\text{CH}_2\text{CO} + \text{H}_2\text{O} + \text{H}$ reaction, it is important to note that $\text{CH}_3\text{COOCOCH}_3$ is present in all the hydrated samples $\text{CH}_2\text{CO}/\text{H}_2\text{O}$. Figure 3.a and 3.b show the IR spectra of $\text{CH}_2\text{CO}/\text{H}_2\text{O}$ ice before and after H-bombardments, respectively. We have detected H_2CO at 1500 and 1728 cm^{-1} , CH_4 at 1304 and 3009 cm^{-1} , and CH_3CHO characterized at 1351 and 1728 cm^{-1} .

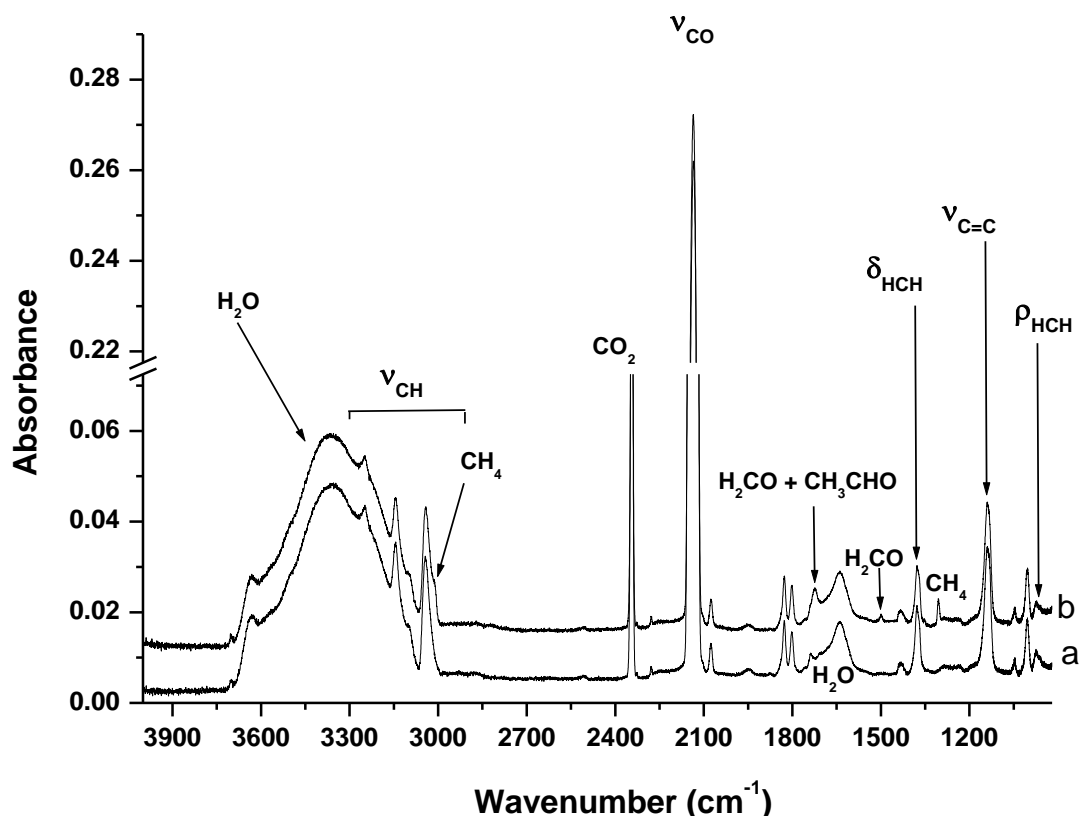


Figure 3. a) IR spectrum of $\text{CH}_2\text{CO}/\text{H}_2\text{O}$ ice formed at 10 K. b) IR spectrum of $\text{CH}_2\text{CO}/\text{H}_2\text{O}$ ice after H-bombardments.

Figure 4.a and 4.b show the resulting difference spectra after and before H-bombardment at 10 K of $\text{CH}_2\text{CO}/\text{H}_2\text{O}$ and pure CH_2CO ices, respectively, in the $2400\text{-}1100\text{ cm}^{-1}$ spectral region. The negative signals are due to the reactants consumed while the positive signals are due to the reaction products formed after hydrogenation. Comparison between Figures 4a and 4b shows that the H-bombardments of $\text{CH}_2\text{CO}/\text{H}_2\text{O}$ ice leads to the same reaction products obtained after H bombardments of pure CH_2CO ice. Consequently, no additional IR signal is detected during the H-bombardment of $\text{CH}_2\text{CO}/\text{H}_2\text{O}$ ice, but only an increase in the yield of CH_4 , H_2CO and CH_3CHO reaction products and in the rate of consumption of ketene as a reactant. In fact, as shown in Figure 4a, for the difference spectrum after and before H-bombardment at 10 K of $\text{CH}_2\text{CO}/\text{H}_2\text{O}$ ice, the IR signals of H_2O and $\text{CH}_3\text{COOCOCH}_3$ remain constant during the hydrogenation process. Therefore, neither H_2O nor $\text{CH}_3\text{COOCOCH}_3$ are consumed during H bombardment of the $\text{CH}_2\text{CO}/\text{H}_2\text{O}$ solid sample.

Comparison of figures 4a and 4b shows that the presence of water in the sample leads to a 3-fold increase in ketene consumption during the hydrogenation process. The reaction products are also formed in large quantities in the presence of water. This shows the catalytic role of H₂O on the CH₂CO + H reaction. However, in comparison with the production of CH₄ and H₂CO, the formation of CH₃CHO appears to be much greater in the CH₂CO/H₂O ice than in the pure CH₂CO ice. Between Figures 4a and 4b, the CH₄ and H₂CO signals are multiplied by about 2, while the CH₃CHO signal at 1351 cm⁻¹, drowned in the noise in Figure 4b, stands out clearly in the presence of water in Figure 4a. For these two experiments relating to the H-bombardment of CH₂CO with and without water, we estimated the quantity of ketene consumed and that of CH₄, H₂CO and CH₃CHO formed by determining the column density *n* (molec cm⁻²) defined as follows:

$$\mathbf{n} = \frac{\ln 10 \int I(\nu) d\nu}{2\varepsilon} \cos(8^\circ)$$

with the integral being the integrated band area (cm⁻¹), ε is the extinction coefficient (cm molec⁻¹) and $\cos(8^\circ)/2$ is a correction term which takes into account the geometry of our IR measurements⁴¹. Table 1 shows the vibrational modes, spectral positions and band strengths considered for the calculations of column densities of CH₂CO, H₂O and reaction products.

Table 1. Vibrational modes, spectral positions and band strengths of CH₂CO, CH₄, H₂CO and CH₃CHO

Molecule	Mode	Position band (cm ⁻¹)	ε (cm molec ⁻¹)	Ref
CH ₂ CO	CH ₂ bend	1376	2.7×10^{-18}	42
	C=O str	2114	1.2×10^{-16}	
H ₂ O	Bend	1657	1.0×10^{-17}	43
	OH-str	3257	2×10^{-16}	
CH ₄	CH ₂ bend	1304	8×10^{-18}	43
	C-H str	3012	1.1×10^{-17}	
H ₂ CO	CH ₂ bend	1500	5.1×10^{-18}	43
	C=O str	1723	1.6×10^{-17}	
CH ₃ CHO	CH ₂ bend	1351	4.5×10^{-18}	44
	C=O str	1728	3×10^{-17}	

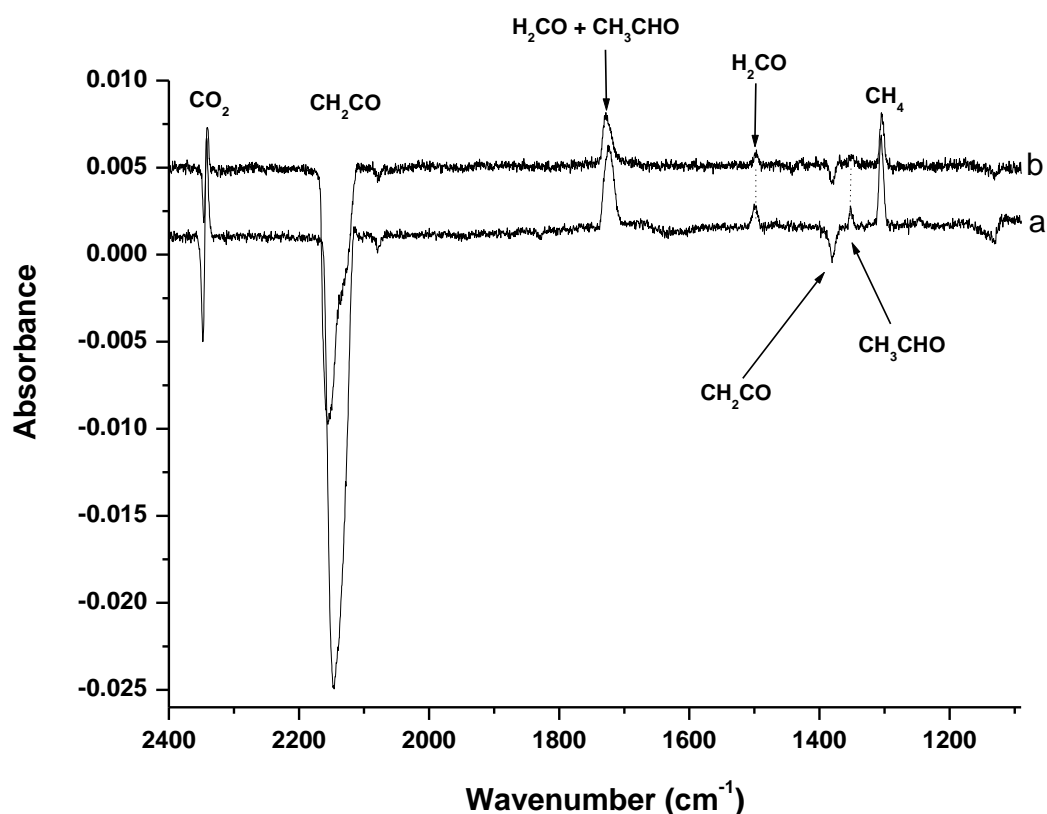


Figure 4: Difference spectrum before and after H-bombardments at 10 K of a) CH₂CO/H₂O ice. b) CH₂CO pure ice. Zoom in 2400-1100 cm⁻¹ spectral region.

Table 2 shows the quantities of ketene consumed and products formed for the CH₂CO + H surface reaction, compared with those obtained for the CH₂CO/H₂O + H surface reaction. For CH₂CO + H surface reaction, the calculation of column density show that the amount of ketene consumed after H-bombardments is 0.5×10^{16} molec cm⁻². For the reaction products, the calculation of column densities shows that the amount of CH₄ formed is 0.31×10^{16} molec cm⁻², for H₂CO is 0.16×10^{16} molec cm⁻² and for CH₃CHO is 0.06×10^{16} molec cm⁻². For the CH₂CO/H₂O + H surface reaction, the CH₂CO consumed after H-bombardments is three time higher than for the pure ketene hydrogenation reaction (1.4×10^{16} vs 0.5×10^{16}). As mentioned above, in the presence of water molecule, the IR signatures of reaction products increase. So, the amount of CH₄ formed increases from 0.31×10^{16} to 0.56×10^{16} molec cm⁻², those of the H₂CO and CH₃CHO increase from 0.16×10^{16} to 0.27×10^{16} molec cm⁻² and from 0.06×10^{16} to 0.18×10^{16} molec cm⁻², respectively.

Table 2. Column densities (molec cm⁻²) of the reaction products formed during CH₂CO+H and CH₂CO/H₂O+H solid state reactions.

	CH ₂ CO H- bombardment	H ₂ O	CH ₂ CO consumed	CH ₄	H ₂ CO	CH ₃ CHO
CH ₂ CO + H surface reaction	2.7×10^{17}	0	0.5×10^{16}	0.31×10^{16}	0.16×10^{16}	0.06×10^{16}
CH ₂ CO/H ₂ O +H surface reaction	1.9×10^{17}	0.8×10^{17}	1.4×10^{16}	0.56×10^{16}	0.27×10^{16}	0.18×10^{16}

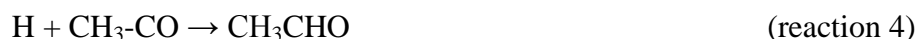
Based on the amounts of CH₂CO consumed during the hydrogenation processes, the CH₂CO + 2H reaction appears to be more efficient in the presence of water. However, if we refer to the yields of reaction products during the hydrogenation of CH₂CO and CH₂CO/H₂O ices, we find that the reaction pathway to form CH₃CHO via the CH₂CO + 2H reaction has the same yield with or without water (12.0% versus 13%). On the other hand, in the presence of water, the yield of CH₄ drops from 62 % to 40% and that of H₂CO from 32% to 19%. These results suggest that water molecules deactivate the reaction pathway to form CH₄ and H₂CO.

4. Discussion

A recent experimental and theoretical study was carried out by our group to investigate the CH₂CO + H solid state reaction under interstellar conditions³⁰. We proposed that ketene molecule reacts with H atoms and leads to the formation of four reaction products, namely CO, H₂CO, CH₄ and CH₃CHO. We showed that CH₃CHO would form through two reaction pathways. The H atom attacks one of the two C atoms of CH₂CO to form CH₃CO or CH₂CHO radicals, then these two radicals react with additional hydrogen atoms to form CH₃CHO. Our calculations have shown that the formation of CH₃CO (reaction 1) and CH₂CHO radicals (reaction 2) presents two different energy barriers of respectively 4.6 and 8.5 kcal/mol, respectively at the CCSD(T)/MP2/cc-PVTZ level (after ZPE correction), close to very recent results²⁹. ~~2.4 and 6.7 kcal/mol at the CCSD(T)/MP2/cc-PVTZ level (4.6 and 8.5 kcal/mol respectively after ZPE correction).~~



This would suggest that CH_3CO radicals would be formed in preference to $\text{H}_2\text{C-CHO}$ through $\text{CH}_2\text{CO} + \text{H}$ under non-energetic conditions. The theoretical calculations showed that $\text{CH}_3\text{CO} + \text{H}$ reaction evolves throughout two barrierless pathways to form CH_3CHO or CO and CH_4 fragments:



In the present work, we try to determine the influence of water molecules in the hydrogen atom reactions on ~~hydrogenation reaction of~~ CH_2CO in solid phase at 10 K. We show in this study that this reaction on ~~the hydrogenation of~~ $\text{CH}_2\text{CO}/\text{H}_2\text{O}$ ice leads to the formation of the same reaction products as obtained with ~~of the hydrogenation of~~ pure CH_2CO ice. From the IR spectra, the amounts of the consumed reactant (CH_2CO) and formed products (CH_4 , H_2CO and CH_3CHO) have been evaluated for the same H-bombardment of ketene ice with and without water. The resulting column densities calculated for $\text{CH}_2\text{CO}/\text{H}_2\text{O} + \text{H}$ and $\text{CH}_2\text{CO} + \text{H}$ surface reactions allow to identify the catalytic role of H_2O in this process ~~the hydrogenation process~~. The solid obtained by co-deposition of water and ketene at 10 K is supposed essentially amorphous. The main difference with the pure ketene ice should be the presence of ketene molecules interacting with a few water molecules. Taken into account the ratio $\text{CH}_2\text{CO}:\text{H}_2\text{O}$ of 2.5 (Table 2), it seems reasonable to study reaction 1 in the presence on one and two water molecules. Several structures of $\text{CH}_2\text{CO},\text{H}_2\text{O}$ (S1) and $\text{CH}_2\text{CO},2\text{H}_2\text{O}$ (S2) close in energy are found. Some of them are displayed in figure 5 together with the corresponding transition states TS1 and TS2. ~~Thus, reaction 1 was studied in the presence of one and two water molecules. The corresponding transition states TS1 and TS2 were characterized, and the activation energies computed with respect to solvated ketene $\text{CH}_2\text{CO},\text{H}_2\text{O}$ and $\text{CH}_2\text{CO},2\text{H}_2\text{O}$, respectively (Figure 5).~~

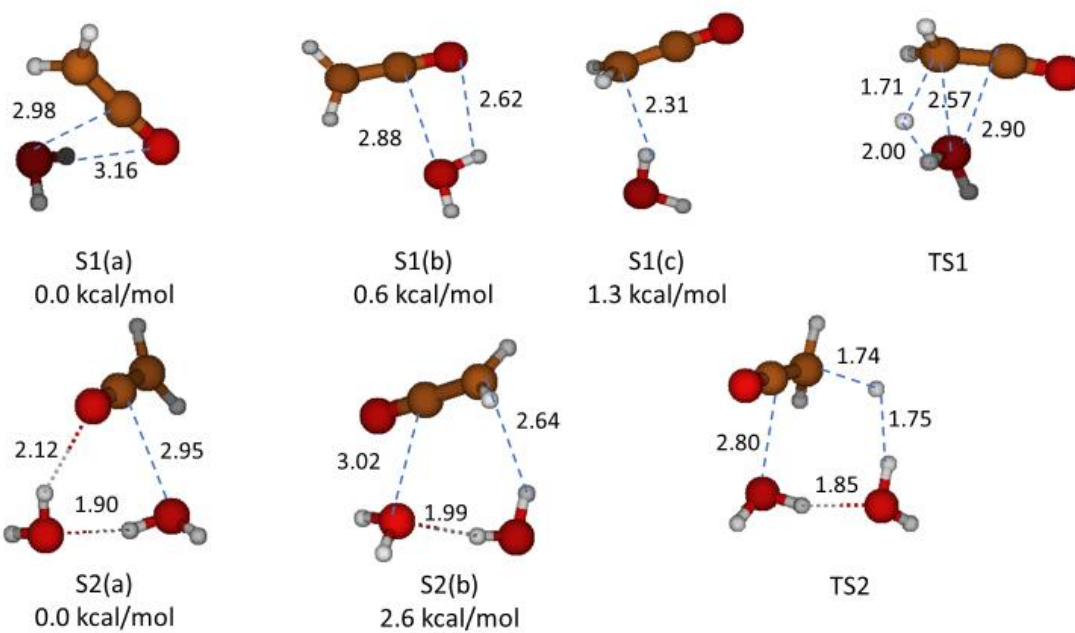
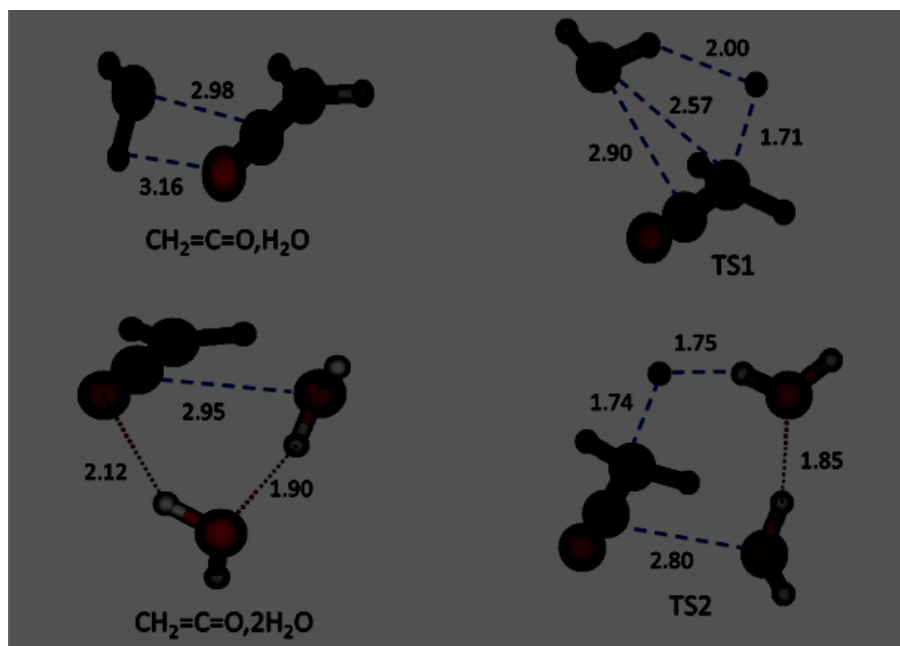


Figure 5: Structures of hydrated ketene (distances in Å) and transition states of H addition. Structures and relative energies of hydrated ketene (distances in Å) and transition states of H addition (CCSD(T)/cc-PVTZ//MP2/ cc-PVTZ).

The activation energies for H addition to ketene in the presence of $n\text{H}_2\text{O}$ ($n = 0, 1, 2$) are reported in Table 3. In Table 3 are reported the potential energy barriers for H addition to ketene in the presence of $n\text{H}_2\text{O}$ ($n = 0, 1, 2$), starting from the most stable ketene, $n\text{H}_2\text{O}$ structure (see figure 5). Indeed, these reactions involve some rearrangement of the system which could be more or less hindered by steric constraints on ice surface. As a result, starting from a higher energy hydrated ketene structures such as S1(b), S1(c) and S2(b) could lower the energy barrier to TS1 and TS2 by 0.6, 1.3, and 2.6 kcal/mol respectively. On the contrary, under other constraints, the reaction could occur by overcoming a barrier higher than TS1 and TS2. Finally, the values reported in Table 3 can be regarded as the mean energy necessary to get the reaction.

Table 3. Activation energy E_a (kcal/mol) of the reaction $\text{H} + \text{H}_2\text{C}=\text{C}=\text{O}, n\text{H}_2\text{O} \rightarrow \text{H}_3\text{C}-\text{CO}$ ($n = 0, 1, 2$) molecules, at the CCSD(T)/MP2/cc_pVTZ (not ZPE corrected) level. Potential energy barriers E_a (kcal/mol) of the reaction $\text{H} + \text{H}_2\text{C}=\text{C}=\text{O}, n\text{H}_2\text{O} \rightarrow \text{H}_3\text{C}-\text{CO}$ ($n = 0, 1, 2$) molecules, at the CCSD(T)/cc_pVTZ//MP2/cc-pVTZ level.

	CH_2CO	$\text{CH}_2\text{CO}, \text{H}_2\text{O}$	$\text{CH}_2\text{CO}, 2\text{H}_2\text{O}$
E_a	2.4	1.1	0.9

	CH_2CO	$\text{CH}_2\text{CO}, \text{H}_2\text{O}$ S1(a)	$\text{CH}_2\text{CO}, 2\text{H}_2\text{O}$ S2(a)
E_a	2.4	1.1	0.9
E_a ZPE corr	4.6	3.8	3.6

These results evidence the catalytic effect of H_2O on this reaction whose potential energy barrier activation energy drops from 4.6 2.4 kcal/mol (without water) to 3.8 and 3.6 1.1 and 0.9 kcal/mol with one and two water molecules, respectively. Water stabilizes the TSs by interaction of one of its hydrogen with the H radical. Indeed, nearby TS distance, the attacking H atom becomes slightly negative (ca. -0.1 a.u.) by a weak electron transfer from the high-lying π HOMO of ketene. It results in a $\text{HO}-\text{H}(\delta^+)\dots\text{H}(\delta^-)$ stabilizing interaction, with a relatively short $\text{H}\dots\text{H}$ distance in the TS. It can be noted that the decrease of the energy barrier is 0.8 kcal/mol by the first water molecule and only 0.2 kcal/mol by the second one: one can guess that a bigger water cluster would not have a significant additional effect.

Another effect of water is to disfavour methane formation (reaction 3). As already mentioned, this reaction is barrierless dealing with isolated $\text{CH}_3\text{-CO}$. We verified that it is always the case with $\text{CH}_3\text{CO}, \text{H}_2\text{O}$ by a scan at the CCSD level, to take into account the singlet diradical character of this system which obviously, it assumes the absence of any obstacle on the reaction path⁴⁵. ~~and we verified that it is always the case with $\text{CH}_3\text{CO}, \text{H}_2\text{O}$.~~ This result thus could originate from steric constraints in interactions of CH_3CO with water molecules of the ice surface. Indeed, reaction 3 needs the approach of H atom in the CH_3 umbrella, near the C-C direction. So, we compared two types of interaction of CH_3CO with three model surfaces: ketene, H_2O and $(\text{H}_2\text{O})_2$ (Figure 6).

Methanal H_2CO is a secondary product of reaction 3 by hydrogenation⁴⁶⁻⁴⁷ of CO. Taking into account that the amount of CO formed is the same as that of CH_4 , Table 2 reveals that about half of CO molecules undergo hydrogenation in both cases: 0.16/0.31 without water vs. 0.56/0.27 with water. The presence of water thus appears to have a negligible effect on the formation of H_2CO .

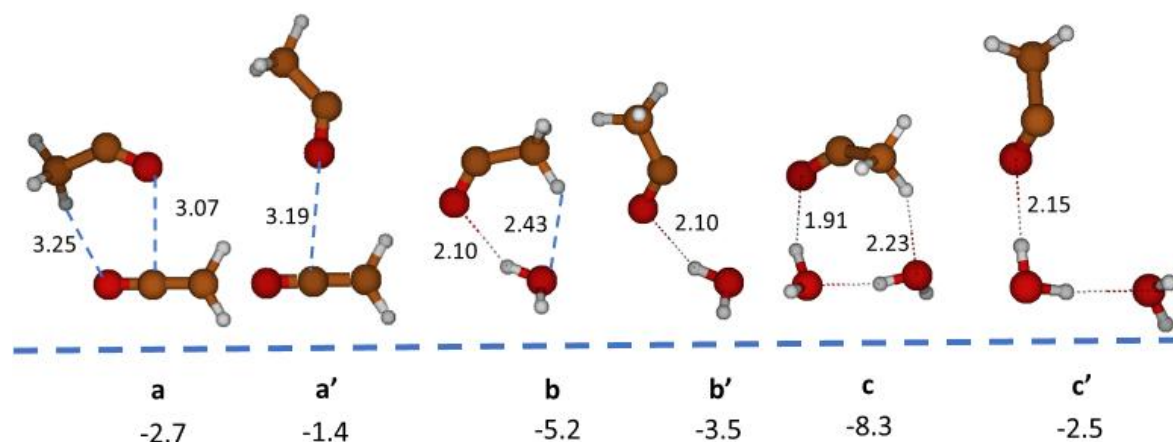


Figure 6: Some geometry interaction of CH_3CO , with ketene and water (distances in Å); interaction energies (kcal/mol) with respect to CH_3CO at infinite separation.

In a first type, a double interaction occurs between CH_3CO and the surface (a, b, c); in a second type, a single interaction occurs (a', b', c'). The interaction energy with respect to CH_3CO at infinite separation is reported for each structure. First, the interactions with ketene (a, a') are relatively weak and one can suppose some “freedom” of CH_3CO on a ketene ice. On the contrary, the interactions with water are significantly greater, especially in double interactions (b, c) which appear sterically less favourable to CH_4 formation.

Conclusions

In the present work, we investigate the influence of water molecules in the solid-phase hydrogenation reaction of CH_2CO at 10 K. We show that the hydrogenation of $\text{CH}_2\text{CO}/\text{H}_2\text{O}$ ice leads to the formation of the same reaction products as the hydrogenation of pure CH_2CO ice. The column densities calculated for the surface reactions $\text{CH}_2\text{CO}/\text{H}_2\text{O} + \text{H}$ and $\text{CH}_2\text{CO} + \text{H}$ underline the catalytic role of H_2O in the hydrogenation process. Based on the quantities of CH_2CO consumed during the hydrogenation processes, the $\text{CH}_2\text{CO} + 2\text{H}$ reaction appears to be more efficient in the presence of water. However, if we refer to the yields of reaction products during the hydrogenation of CH_2CO and $\text{CH}_2\text{CO}/\text{H}_2\text{O}$ ices, we find that the reaction pathway to form CH_3CHO via the $\text{CH}_2\text{CO} + 2\text{H}$ reaction has the same yield with or without water while those of CH_4 and H_2CO drop considerably. Our experimental results suggest that even if they have a catalytic role during the hydrogenation of CH_2CO , water molecules tend to deactivate the reaction pathway leading to CH_4 , CO , and H_2CO . Our theoretical calculations show that the intermediate reaction CH_3CO radicals would be formed in preference to $\text{H}_2\text{C-CHO}$ through the H-addition reaction $\text{CH}_2\text{CO} + \text{H}$. Then $\text{CH}_3\text{CO} + \text{H}$ reaction evolves throughout two barrierless pathways to form (CH_3CHO) or (CO , H_2CO and CH_4). The catalytic effect of H_2O on the $\text{CH}_2\text{CO} + \text{H}$ reaction is highlighted through the calculation of the potential energy barrier ~~activation energy~~ which drops from 4.6 kcal/mol (without water) to 3.8 and 3.6 kcal/mol with one and two water molecules, respectively. The effect of water on reducing methane formation is mainly attributed to steric constraints in the interactions of CH_3CO with water molecules. The $\text{H}_2\text{O-CH}_3\text{CO}$ interaction is considerably greater, which seems sterically less favorable to the formation of fragments such as CO and CH_4 .

References

1. M. Ibrahim, J. C. Guillemin, L. Krim, MNRAS, 2022, **514**, 3754–3764
2. R. L. Hudson, M. J. Loeffler, ApJ, 2013, **773**, 109
3. A. M. Turner, A. S. Koutsogiannis, N. F. Kleimeier, A. Bergantini, C. Zhu, R. C. Fortenberry, R. I. Kaiser, ApJ, 2020, **896**, 88
4. K. Chuang, G. Fedoseev, C. Scirè, G. A. Baratta, C. Jager, Th. Henning, H. Linnartz, and M. E. Palumbo, A&A, 2021, **650**, A85
5. K.-J., Chuang, G. Fedoseev, S. Ioppolo, E. F. van Dishoeck, H. Linnartz, , MNRAS, 2016, **455**, 1702
6. G. Fedoseev , D. Qasim, K. Chuang, S. Ioppolo, T. Lamberts, E. F. Van Dishoeck, and H. Linnartz, AJ, 2022, **924**:110 (8pp)
7. I.-C. Chen, W. H. Green Jr, C. B. Moore, 1988, J. Chem. Phys., 1988, **89**, 314
8. I.-C. Chen, C. B. Moore, J. Phys. Chem., 1990a, **94**, 263
9. I.-C. Chen, C. B. Moore, J. Phys. Chem., 1990b, **94**, 269
10. Turner, B., ApJL, 1977, **213**, L75.
11. L. Johansson, C. Andersson, J. Ellder, P. Friberg, A. Hjalmarsen, B. Hoglund, W. M. Irvine, H. Olofsson, and G. Rydbeck, , A&A, 1984, **130**, 227
12. W. M. Irvine, P. Friberg, N. Kaifu, K. Kawaguchi, Y. Kitamura, H. E. Matthews, ApJ, 1989, **342**, 871-875
13. B. Turner, R. Terzieva, & E. Herbst, ApJ, 1999, **518**, 699
14. A. Bacmann, V. Taquet, A. Faure, C. Kahane, C. & Ceccarelli, A&A, 2012, **541**, L12
15. S. Muller, A. Beelen, M. Guélin, S. Aalto, J. H. Black, F. Combes, S. J. Curran, P. Theule, and S. N. Longmore, A&A, 2011, **535**, A103
16. M. H. Moore, R. L. Hudson, ICARUS, 1998, **135**, 518–527
17. L. Krim , J. Lasne, C. Laffon, P. Parent, J. Phys. Chem. A., 2009, **113**, 8979-8984
18. K. I. Öberg, E. F. van Dishoeck, H. Linnartz, and S. Andersson, AJ, 2010, **718**, 832–840
19. C. Pirim, L. Krim, Chemical Physics, 2011, **380**, 67-76
20. M. Jonusas, L. Krim, MNRAS, 2017, **470**, 4564–4572
21. M. Bulak, D. M. Paardekooper, G. Fedoseev, and H. Linnartz, A&A, 2021, 647, A82
22. P. S. Peters, D. Duflot, A. Faure, C. Kahane, C. Ceccarelli, L. Wiesenfeld, and C. Toubin, J. Phys. Chem. A, 2011, **115**, 8983–8989
23. Z. P. Nhlabatsi, P. Bhasi and S. Sitha, Phys. Chem. Chem. Phys., 2016, **18**, 20109
24. N. Darla, D. Sharma, and S. Sitha, J. Phys. Chem. A, 2020, **124**, 165-175
25. L. Zamirri, P. Ugliengo, C. Ceccarelli, A. Rimola ACS Earth Space Chem. 2019, **3**, 1499–1523
26. A. Rimola, M. Sodupe, P. Ugliengo, Phys. Chem. Chem. Phys., 2010, **12**, 5285–5294

27. A. Rimola, D. Skouteris, N. Balucani, C. Ceccarelli, J. Enrique-Romero, V. Taquet, P. Ugliengo, *ACS Earth Space Chem.* 2018, **2**, 720–734.
28. D. E. Woon, *Int. J. Quantum Chem.*, 2002, **88**, 226–235.
29. S. Ferrero, C. Ceccarelli, P. Ugliengo, M. Sodupe, A. Rimola, *ApJ*, 2023, **951**, 150.
30. M. Ibrahim, J. C. Guillemin, P. Chaquin, A. Markovits and L. Krim, *Phys. Chem. Chem. Phys.*, 2022, **24**, 23245-23253
31. Jonusas M., Krim L., *MNRAS*, 2016, **459**, 1977
32. (Ref) Gaussian 09, Revision A.01, M. J. Frisch, G. W. Trucks, H. B. Schlegel, G. E. Scuseria, M. A. Robb, J. R. Cheeseman, G. Scalmani, V. Barone, B. Mennucci, G. A. Petersson, H. Nakatsuji, M. Caricato, X. Li, H. P. Hratchian, A. F. Izmaylov, J. Bloino, G. Zheng, J. L. Sonnenberg, M. Hada, M. Ehara, K. Toyota, R. Fukuda, J. Hasegawa, M. Ishida, T. Nakajima, Y. Honda, O. Kitao, H. Nakai, T. Vreven, J. A. Montgomery, Jr., J. E. Peralta, F. Ogliaro, M. Bearpark, J. J. Heyd, E. Brothers, K. N. Kudin, V. N. Staroverov, R. Kobayashi, J. Normand, K. Raghavachari, A. Rendell, J. C. Burant, S. S. Iyengar, J. Tomasi, M. Cossi, N. Rega, J. M. Millam, M. Klene, J. E. Knox, J. B. Cross, V. Bakken, C. Adamo, J. Jaramillo, R. Gomperts, R. E. Stratmann, O. Yazyev, A. J. Austin, R. Cammi, C. Pomelli, J. W. Ochterski, R. L. Martin, K. Morokuma, V. G. Zakrzewski, G. A. Voth, P. Salvador, J. J. Dannenberg, S. Dapprich, A. D. Daniels, Ö. Farkas, J. B. Foresman, J. V. Ortiz, J. Cioslowski, D. J. Fox, Gaussian, Inc., Wallingford CT, **2009**.
33. C B. Moore, G. C., Pimentel, *JCP*, 1963, **38**, 2816
34. W. D Allen,., & H. F., Schaefer, III, *JCP*, 1986, **81**, 2212
35. Hudson, R. L., & Moore, M. H. 2000, *Icarus*, 145, 661
36. Bennett, C. J., Chen, S.-J.; Sun, B.-J., Chang, A. H. H., Kaiser R. I., 2007a, *ApJ*, 660, 1588
37. Chapados C., Cabana A., 1972, *Can. J. Chem.*, 50, 3521
38. Gálvez Ó., Maté B., Herrero V. J., Escribano R., 2009, *ApJ*, 703, 2101
39. Hudson R. L., Ferrante R. F., 2020, *MNRAS*, 492, 283
40. T. F. Kahan, T. K. Ormond, G. B. Ellison, V. Vaida, *Chemical Physics Letters*, 2013, **565**, 1-4
41. C. J. Bennett, C. Jamieson, A. M. Mebel, R. I. Kaiser, *PCCP*, 2004, **6**, 735
42. O. Berg, G. E. Ewing, *JPhCH*, 1991, **95**, 2908
43. M. Bouilloud, N. Fray, Y. Benilan, H. Cottin, M.-C. Gazeau and A. Jolly, *MNRAS*, 2015, **451**, 2145-2160
44. C. J. Bennett, C. Jamieson, Y. Osamura, and R. I. Kaiser, *ApJ*, 2005, **624**, 1097-1115
45. J. Perrero, P. Ugliengo, C. Ceccarelli, A. Rimola, 2023, *MNRAS*, **525**, 2654–2667
46. A. G. G. M. Tielens, W. Hagen, 1982, *A&A*, **114**, 245-253
47. N. Tieppo, F. Pauzat, O. Parisel, Y. Ellinger, 2023, *MNRAS*, **518**, 3820-3823.

